Journal of Alzheimer's Disease 84 (2021) 1351–1362
DOI 10.3233/JAD-215160
IOS Press

Characterizing the Resilience Effect of Neurodegeneration for the Mechanistic Pathway of Alzheimer's Disease

Di Hu[a], Chuning Liu[a], Kai Xia[b], Amy Abramowitz[b], Guorong Wu[b,c,*] and Alzheimer's Disease Neuroimaging Initiative (ADNI)[1]
[a]*Department of Biostatistics, University of North Carolina at Chapel Hill, Chapel Hill, NC, USA*
[b]*Department of Psychiatry, University of North Carolina at Chapel Hill, Chapel Hill, NC, USA*
[c]*Department of Computer Science, University of North Carolina at Chapel Hill, Chapel Hill, NC, USA*

Accepted 13 September 2021
Pre-press 13 October 2021

Abstract.
Background: With the rapid development of neurobiology and neuroimaging technologies, mounting evidence shows that Alzheimer's disease (AD) is caused by the build-up of two abnormal proteins, amyloid-β plaques (A) and neurofibrillary tangles (T). Over time, these AD-related neuropathological burdens begin to spread throughout the brain, which results in the characteristic progression of symptoms in AD.
Objective: Although tremendous efforts have been made to link biological indicators to the progression of AD, limited attention has been paid to investigate the multi-factorial role of socioeconomic status (SES) in the prevalence or incidence of AD. There is high demand to explore the synergetic effect of sex and SES factors in moderating the neurodegeneration process caused by the accumulation of A and T biomarkers.
Methods: We carry out a meta-data analysis on the longitudinal neuroimaging data, clinical outcomes, genotypes, and demographic data in Alzheimer's Disease Neuroimaging Initiative (ADNI) database (http://adni.loni.usc.edu).
Results: Our major findings include 1) education and occupation show resilience effects at the angular gyrus, superior parietal lobule, lateral occipital-temporal sulcus, and posterior transverse collateral sulcus where we found significant slowdown of neurodegeneration due to higher education level or more advanced occupation rank; 2) A and T biomarkers manifest different spatial patterns of brain resilience; 3) *BDNF* (brain-derived neurotrophic factor) single nucleotide polymorphism (SNP) *rs10835211* shows strong association to the identified resilience effect; 4) the identified resilience effect is associated with the clinical manifestation in memory, learning, and organization performance.
Conclusion: Several brain regions manifest resilience from SES to A and T biomarkers. *BDNF* SNPs have a potential association with the resilience effect from SES. In addition, cognitive measures of learning and memory demonstrate the resilience effect.

Keywords: Alzheimer's disease, cognitive reserve, computational proxy, neurodegeneration

INTRODUCTION

Alzheimer's disease (AD) is a common neurodegenerative disorder with characteristic pathologic changes. Although the underlying pathophysiological mechanism of AD progression is largely elusive, the underlying pathologic processes can be documented by postmortem examination or *in vivo* by biomarkers [1, 2]. The most commonly used biomarkers in research and clinic areas include amyloid-β

*Correspondence to: Guorong Wu, PhD, Department of Psychiatry, University of North Carolina at Chapel Hill, Chapel Hill, NC 27599, USA. Tel.: +1 919 966 2216; E-mail: grwu@med.unc.edu.

[1]Data used in preparation of this article were obtained from the Alzheimer's Disease Neuroimaging Initiative (ADNI) database (https://adni.loni.usc.edu). As such, the investigators within the ADNI contributed to the design and implementation of ADNI and/or provided data but did not participate in analysis or writing of this report. A complete listing of ADNI investigators can be found at: https://adni.loni.usc.edu/wp-content/uploads/how_to_apply/ADNI_Acknowledgement_List.pdf.

(Aβ) deposition, pathologic tau, and neurodegeneration (such as cortical thickness), which constitute the backbone of the A-T-N research framework of AD [1].

The rapid development of neuroimaging technologies enables *in vivo* measurement of the pathologic burden using biomarkers. For example, Aβ plaques and fibrillar tau can be quantified at different brain regions through the cortical Aβ-PET and tau-PET ligand binding, respectively [3]. Biomarkers of neurodegeneration or neuronal injury include cerebrospinal fluid (CSF) tau, fluorodeoxyglucose (FDG)-PET hypometabolism, and atrophy on MRI [3]. In the recent A-T-N research framework, the most popular hypothesis of the mechanistic pathway is that amyloidosis induces or facilitates the spread of pathologic tau, which is immediately proximate to neurodegeneration [4].

The preservation of normal cognition despite underlying neuropathology has been termed resilience. Converging evidence shows that cognitive decline is not only regulated by the abnormal deposition of Aβ or tau, but also potentially moderated by the brain's ability to maintain normal cognition [5–7]. Brain resilience has been quantified in various ways. For example, the operational measure of the brain reserve [8] is defined as the standardized individual difference between the observed and predicted gray matter volume. Recently, intelligence quotient (IQ) was used as a proxy for cognitive reserve [9], where high premorbid IQ was linked to lower cognitive age independent of brain age. In our previous work [10], we presented a regression model to investigate this cognitive reserve proxy, where the response is the severity of AD progression and the predictors include age, sex, pathology burden, education, AD polygenic risk score, and their interactions. Our hypothesis was that the counteracting effect size of the joint product of AD pathology (measured by tau/$A\beta_{42}$ ratio) and socioeconomic status (SES) factors (measured by educational level and occupation level) moderates cognitive decline and can be used as the computational proxy of cognitive reserve. Given this new proxy of cognitive reserve, we found that the high education group has more resilience to AD pathology than the low education group, however, at the expense of faster cognitive decline after the neuropathology burden is beyond the tipping point.

Although significant efforts have been made to characterize cognitive resilience by investigating the relationship between clinical outcome and neuropathology burden, few studies have examined the characteristics of resilience at different brain regions. In the current study [10], we propose a model for a proxy measurement of resilience at the pathological biomarker level. This model includes the joint effect of sex and SES moderators. Our regression model predicts the degree of future neurodegeneration found on FDG-PET scan using the baseline Aβ or tau biomarker, where age, sex, SES factors, and the sex-by-SES interaction are confounding variables. Similar to our previous work [8], we further characterize resilience at each brain region which allows us to investigate the spatial patterns of cognitive reserve in the brain. For the brain regions showing a significant resilience effect, we conduct 1) upstream association with genotypes to explore the genetic factors that may account for the resilience; and 2) downstream association with clinical outcomes. As multiple lines of evidence show that women are at greater risk for both developing AD and having more severe pathology after age 65 [11], we go one step further to examine whether the identified resilience effects manifest sex-specific differences.

All the meta-data analyses are performed on genotype data, neuroimaging data, and demographic data from Alzheimer's Disease Neuroimaging Initiative (ADNI) database. We find there are a moderate number of regions showing resilience to either Aβ and tau pathology. However, there is no brain region showing resilience to both Aβ and tau pathology. We find one single nucleotide polymorphism (SNP), *rs10835211*, in the brain-derived neurotrophic factor (*BDNF*) gene family has a strong association with the identified resilience effect, indicating the beneficial influence of neuroplasticity on the brain resilience observed at the pathological level. Downstream association between the identified resilience effect and clinical outcomes reveals that the clinical manifestations on learning, memory, and organization are closely related to the resilience effect. Sex difference of resilience effect has not been detected either for Aβ or tau pathology.

MATERIALS AND METHODS

Data descriptions

The data used in our study were obtained from the ADNI database (http://www.ida.loni.usc.edu). ADNI seeks to develop biomarkers, advance the understanding of AD pathophysiology, improve diagnostic methods for early detection of AD. Additional goals are examining the rate of progress for both mild cog-

nitive impairment (MCI) and AD, as well as building a large repository of clinical and imaging data. ADNI enrolls participants between the ages of 55 and 90 who are recruited at 57 sites in the United States and Canada. After obtaining informed consent, participants undergo a series of initial tests that are repeated at intervals over subsequent years, including clinical evaluation, neuropsychological tests, genetic testing, lumbar puncture, and MRI and PET scans. There are four phases of the ADNI study (ADNI1, ADNI-GO, ADNI2, and ADNI3). Some participants were carried forward from previous phases for continued monitoring, while new participants were added with each phase to further investigate the evolution of AD.

Regarding the neuropathological imaging data, the concentration level of Aβ, tau, and metabolism neurodegeneration biomarker can be measured using Aβ-PET, tau-PET, and FDG-PET, respectively. In this study, we use Destrieux atlas [12] which consists of 148 cortical regions. For each PET image, we apply a set of image processing steps to calculate the average SUVR (standardized uptake value ratio) for each region. Note, SUVR is the most common quantitative method used to make regional comparisons within a subject as well as between subjects and computed as the degree of radiotracer uptake in a target region of interest with respect to a reference region. The data processing pipeline includes 1) skull stripping, 2) segmenting tissue into white matter, grey matter, and CSF, 3) registering to the underlying image, and 4) calculating the SUVR degree for each ROI which is normalized by the whole cerebellum reference. We further visualize the average regional SUVR of Aβ and matched FDG-PET in the left panel of Fig. 1. Likewise, we display the average regional SUVR of tau and the matched FDG-PET in the right panel of Fig. 1.

Regarding the SES data, the years of education and occupations were recorded in the ADNI database in recruiting subjects. We classified education and occupation as the same criteria used in Lo's study [13]. Years of Education were divided into three categories: high (years of education > 17 years), intermediate (years of education 15–17 years), and low (years of education<15 years). The occupation considered is the one that the subject performed during most of his/her adult life or with the longest time of service. The occupation level was classified into three groups according to the National Statistics Socio-economic classification [14]: 1) high level (professional or managerial), 2) intermediate level (skilled), and 3) low level (partly skilled or unskilled).

Regarding the genotype data, we calculated the AD-related polygenic risk score (PRS) for each subject. First, we filtered the SNP in the GWAS results in CTG lab (https://ctg.cncr.nl/software/summary_statistics) by MAF greater than 0.01. Then, the SNPs were LD pruned with $r^2 = 0.1$ in a 1000 kb window, 324,982 SNPs were left after the pruning. And we utilized PLINK 1.9 to calculate the weighted PRS of Alzheimer's disease using SNPs with AD association of $p < 10^{-4}$.

Regarding the demographic data, we show the age and gender information of participants in Table 1. Since we measure the resilience specific to the Aβ-to-neurodegeneration (A-N) and tau-to-neurodegeneration (T-N) mechanism pathways separately, each subject is required to have imaging data from two modalities. There are 1,086 subjects who have both Aβ-PET and FGD-PET data and 346 subjects who have both tau-PET and FGD-PET data. For participants in the A-N model, the average age is 72.8 years old, 53.9% are male, 60.7% have a professional or managerial occupation, and 38.9% have years of education longer than 17 years. For participants in the T-N model, the average age at baseline is 71.4 years old, 54.3% are male, 65.3% have the professional or managerial occupation, and 42.8% have years of education longer than 17 years.

Regarding the clinical outcome data, there are 22 items in clinical data (Table 2), including Rey's

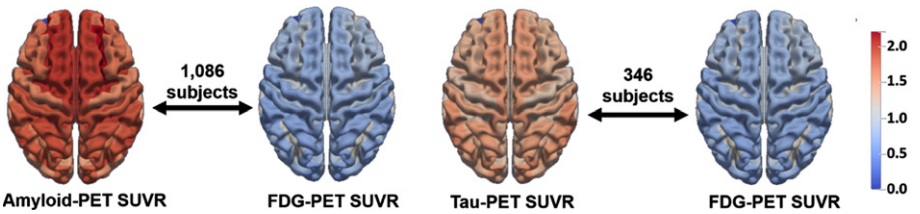

Fig. 1. Left: The average regional SUVR degree of Aβ and the matched FDG-PET from 1,086 subjects. Right: The average regional SUVR degree of tau and matched FDG-PET image from 346 subjects.

Table 1
Demographic characteristics of participants in A-N and T-N models

Resilience models	A-N resilience (*N* = **1,086**)	T-N resilience (*N* = 346)
Age	72.8 (7.20)	71.4 (7.00)
Gender		
Male	585 (53.9%)	188 (54.3%)
Female	501 (46.1%)	158 (45.7%)
Occupation		
Low	84 (7.7%)	22 (6.4%)
Medium	343 (31.6%)	98 (28.3%)
High	659 (60.7%)	226 (65.3%)
Education		
Low	309 (28.5%)	94 (27.2%)
Medium	355 (32.7%)	104 (30.1%)
High	422 (38.9%)	148 (42.8%)

*Data are in mean (SD) for continuous variables and in (%) for categorical variables.

Auditory Verbal Learning Test (RAVLT) scores, Logical Memory test, Trail Making Test, and Everyday Cognition (Ecog) scales (self-reported/study partner reported). We matched the clinical data to our imaging data. There are 1,016 participants with both Aβ-PET and clinical outcome data, and 331 participants with both tau-PET and clinical outcome data.

Statistical analysis

We first present a set of statistical models to identify and quantify resilience at each brain region by examining the relationship of Aβ and tau biomarkers. We specifically model the joint effect of sex and SES factors in our model, which allows us to understand the moderating factors behind the neuropathology. For the regions showing resilience to the development of neurodegeneration, we will examine the association with genotype of the BDNF gene and clinical outcomes using sparse canonical correlation analysis (sCCA) [15].

Identify and quantify resilience effect of neurodegeneration

Rationale

There is a converging consensus that Aβ and tau biomarkers are two major reasons for neurodegeneration in the current A-T-N research framework [1]. In general, the brain manifests more and more severe neurodegeneration patterns as the level of A and T biomarkers increase. On the flip side, it is quite common in the clinic that some individuals maintain cognitive normal even the A-T-N biomarker level is beyond the diagnostic cut-offs [7]. Along with our previous work [10], many cognitive reserve studies regard SES factors as the proxy of measuring cognitive reserve [16]. In this paper, we extend the statistical model in [10] to characterize the A/T-specific resilience effect of neurodegeneration at each brain region. Specifically, we opt to predict the regional degree of N biomarker (using FGD-PET) at the follow-up scan (2-3 years after)

Table 2
The summary of 22 itemized clinical outcomes

Outcome Name	Description	Mean (SD)
RAVLT_immediate	RAVLT Immediate	37.9 (12.7)
RAVLT_learning	RAVLT Learning	4.75 (2.71)
RAVLT_forgetting	RAVLT Forgetting	4.33 (2.82)
RAVLT_perc_forgetting	RAVLT Percent Forgetting	53.2 (39.5)
LDELTOTAL	Logical Memory - Delayed Recall	8.73 (5.32)
TRABSCOR	Time to Complete Trail Making Test	111 (68.0)
FAQ	Functional Activities Questionnaire Total Score	3.53 (5.87)
MOCA	Montreal Cognitive Assessment	23.3 (3.95)
EcogPtMem	Participant ECog - Mem	2.09 (0.718)
EcogPtLang	Participant ECog - Lang	1.72 (0.621)
EcogPtVisspat	Participant ECog - Vis//Spat	1.37 (0.516)
EcogPtPlan	Participant ECog - Plan	1.40 (0.542)
EcogPtOrgan	Participant ECog - Organ	1.52 (0.611)
EcogPtDivatt	Participant ECog - Div atten	1.80 (0.733)
EcogPtTotal	Participant ECog - Total	1.67 (0.523)
EcogSPMem	Study Partner ECog - Mem	2.06 (0.925)
EcogSPLang	Study Partner ECog - Lang	1.62 (0.732)
EcogSPVisspat	Study Partner ECog - Vis//Spat	1.47 (0.703)
EcogSPPlan	Study Partner ECog - Plan	1.58 (0.790)
EcogSPOrgan	Study Partner ECog - Organ	1.67 (0.873)
EcogSPDivatt	Study Partner ECog - Div atten	1.86 (0.937)
EcogSPTotal	Study Partner ECog - Total	1.71 (0.739)

using the baseline A/T biomarker level. In addition to the confounders such as age and sex, we model the joint effect of A/T biomarkers and SES factors in our model. In this regard, we conceptualize the mechanism of A/T-specific resilience as a joint product of neuropathological burden and socioeconomic factors, where the resistant effect can be captured by estimating the counteracting relationship between N and A/T biomarkers.

Statistical model

Suppose we have the regional A/T biomarker and N biomarker for in total P subjects. We parcellate each brain into Q regions. We apply the following linear regress model at each brain region R_j ($j = 1, \ldots, Q$), where the response is the N biomarker $y_N^{i,j}$ ($i = 1, \ldots, P$) measured from the FDG-PET image. One major predictor is the regional A or regional T biomarker $x_{A/T}^{i,j}$. Since we categorize education and occupation into low, middle, and high levels, we include $x_{Mid\_Edu}^i$ and $x_{High\_Edu}^i$ for the relative education level (with respect to the low education group) while $x_{Mid\_Occu}^i$ and $x_{High\_Occu}^i$ for the relative occupation category (with respect to the low skilled group). Here, age x_{age}^i, sex x_{sex}^i, and AD-PRS x_{PRS}^i are considered as confounding variables. Furthermore, the interaction effect term consists of SES factors, and A/T biomarker value. Thus, we have four instances of the joint effect term given the combination of two neuropathology biomarkers (A or T) and two SES factors (either education or occupation level). To simplify, we present the following four regression models with respect to different joint effect terms:

- **A-specific resilience from education:**

$$y_N^{i,j} = \beta_0 + \beta_1 x_A^{i,j} + \beta_2 x_{sex}^i + \beta_3 x_{PRS}^i + \beta_4 x_{Age}^i + \beta_5 x_{Mid\_Edu}^i + \beta_6 x_{High\_Edu}^i + \beta_7 x_{Mid\_Occu}^i + \beta_8 x_{High\_Occu}^i + \beta_9 \left(x_A^{i,j} \cdot x_{Mid\_Edu}^i\right) + \beta_{10} \left(x_A^{i,j} \cdot x_{High\_Edu}^i\right) + \varepsilon^{i,j} \quad (1)$$

- **A-specific resilience from occupation:**

$$y_N^{i,j} = \beta_0 + \beta_1 x_A^{i,j} + \beta_2 x_{sex}^i + \beta_3 x_{PRS}^i + \beta_4 x_{Age}^i + \beta_5 x_{Mid\_Edu}^i + \beta_6 x_{High\_Edu}^i + \beta_7 x_{Mid\_Occu}^i + \beta_8 x_{High\_Occu}^i + \beta_9 \left(x_A^{i,j} \cdot x_{Mid\_Occu}^i\right) + \beta_{10} \left(x_A^{i,j} \cdot x_{High\_Occu}^i\right) + \varepsilon^{i,j} \quad (2)$$

- **T-specific resilience from education:**

$$y_N^{i,j} = \beta_0 + \beta_1 x_T^{i,j} + \beta_2 x_{sex}^i + \beta_3 x_{PRS}^i + \beta_4 x_{Age}^i + \beta_5 x_{Mid\_Edu}^i + \beta_6 x_{High\_Edu}^i + \beta_7 x_{Mid\_Occu}^i + \beta_8 x_{High\_Occu}^i + \beta_9 \left(x_T^{i,j} \cdot x_{Mid\_Edu}^i\right) + \beta_{10} \left(x_T^{i,j} \cdot x_{High\_Edu}^i\right) + \varepsilon^{i,j} \quad (3)$$

- **T-specific resilience from occupation:**

$$y_N^{i,j} = \beta_0 + \beta_1 x_T^{i,j} + \beta_2 x_{sex}^i + \beta_3 x_{PRS}^i + \beta_4 x_{Age}^i + \beta_5 x_{Mid\_Edu}^i + \beta_6 x_{High\_Edu}^i + \beta_7 x_{Mid\_Occu}^i + \beta_8 x_{High\_Occu}^i + \beta_9 \left(x_T^{i,j} \cdot x_{Mid\_Occu}^i\right) + \beta_{10} \left(x_T^{i,j} \cdot x_{High\_Occu}^i\right) + \varepsilon^{i,j} \quad (4)$$

Given the evidence regarding AD pathogenesis, we posit that regional A/T resilience should be meet the following two criteria: (1) The pathology burden $x_{A/T}^{i,j}$ shows significant contribution to the neurodegeneration at the underlying region. Since lower metabolism level $y_N^{i,j}$ and higher neuropathological degree $x_{A/T}^{i,j}$ indicate high risk of developing AD, we expect the sign of β_1 is negative and the biomarker term $x_{A/T}^{i,j}$ shows significance without the interaction term. (2) Since resilience is defined as the moderation effect against neurodegeneration, we expect the sign of β_9 or β_{10} is positive and the associated joint effect term shows significance. By applying the above four statistical models to each brain region, we are able to not only identify whether the underlying regions manifest A/T-specific resilience effects but also understand the driving SES factors behind the resilience.

Suppose one of the joint-effect terms meets the above two criteria in either regression model in Eq. 1–4 at the region R_j. Then, we can calculate the resilience effect for each subject by multiplying the value of the joint term and the corresponding estimated effect size. With slight abuse of notation, we use y_{res}^i to denote the individual-based resilience effect for i^{th} subject for one specific type (either A to T) of resilience effects at the specific regions.

Genetic association with neuroplastic related genetic markers

There is accumulating evidence that the BDNF gene acts in a protective role and may moderate the neurodegeneration process in AD [17, 18]. In

this context, we use the candidate gene approach to investigate the association between the A/T-specific resilience effect and the SNPs in the BNDF gene, which allows us to discover the genetic factors associated with the identified resilience effect.

To avoid the cost of genome-wide multiple comparisons, we only focus our analysis on several commonly-reported SNPs in BDNF [19]. The following linear regression model was used to explore the association between the A/T-specific resilience effect y^i_{res} and each BDNF SNP x_{SNP}, separately. To adjust for the population stratification, we further add the first three principal components of SNPs into the model as:

$$y^i_{res} = \beta_0 + \beta_1 x_{SNP} + \beta_2 x_{PC1} + \beta_3 x_{PC2} + \beta_4 x_{PC3} + \varepsilon^i \quad (5)$$

where x_{PC1}, x_{PC2}, and x_{PC3} are the first three principal components, respectively.

Linking multiple domains of clinical symptom to the identified resilience effect

Suppose we have identified p resilience effects for each subject, including all possible resilience from Equation 1 to Equation 4. Each subject also has q clinical outcome measures. Thus, given n subjects, we can form a data matrix of resilience effects $\mathbf{X} \in \mathcal{R}^{n\times p}$ and another data matrix of clinical measurements $\mathbf{Y} \in \mathcal{R}^{n\times q}$. We use CCA to jointly align $\mathbf{X}$ and $\mathbf{Y}$ by estimating the loading vectors $\mathbf{u} \in \mathcal{R}^{p\times d}$ and $\mathbf{v} \in \mathcal{R}^{q\times d}$ such that the transformed data matrix $\mathbf{Xu}$ and $\mathbf{Yv}$ have the largest correlation degree, where $d \leq \min(p, q)$. To make it easier to interpret the result, we further add ℓ_1-norm sparsity constraint on $\mathbf{u}$ and $\mathbf{v}$, where the objective function is represented as:

$$\arg\max_{u,v} \mathbf{u^T X^T Y v}, \text{ subject to } \|\mathbf{u}\|_2^2 \leq 1, \|\mathbf{v}\|_2^2 \leq 1, \|\mathbf{u}\|_1 \leq c_1, \mathbf{v}_1 \leq c_2, \quad (6)$$

where c_1 and c_2 are scalar variables controlling the strength of sparsity. $\mathbf{u}$ and $\mathbf{v}$ can be solved by [20]. In this study, we focus on the loading vectors $\mathbf{v}$ since each column in $\mathbf{v}$ describes one combination of clinical vectors that links with the resilience effects. Similar to applying PCA (principle component analysis) for dimension reduction, the first column vector in $\mathbf{v}$ (associated with the largest Eigenvalue of $\mathbf{X^T Y}$) describes the dimension that explains largest variations in $\mathbf{Yv}$ that links with $\mathbf{u^T X^T}$ in the latent common space, and so on.

We conduct a grid search in increment of 0.1 to determine the combination of parameters (i.e., c_1 and c_2) that would yield the highest canonical correlation of the first variate across ten randomly resampled samples, each consisting of two-thirds of the full dataset. Then, we apply a 1000-times permutation testing procedure to assess the statistical significance of each canonical variate. Here, we hold the resilience matrix constant and then shuffled the rows of the clinical matrix so as to break the linkage of resilience and clinical features. Then we performed sCCA using the same set of regularization parameters to generate a null distribution of correlation after 1000-time permutation procedure. The p-value (P_{perm}), was estimated as the number of null correlations (r_i) that exceed the average sCCA correlations estimated on the original dataset ($\bar{r}$), with false discovery rate correction across the top canonical variates selected by scree plot:

$$P_{perm} = \frac{\sum_{i=1}^{1000} \begin{cases} 1, if & r_i \geq \bar{r} \\ 0, if & r_i \leq \bar{r} \end{cases}}{1000} \quad (7)$$

To further select clinical features that consistently contributed to each canonical variate, we performed a 1000-times bootstrap resampling procedure. Features whose 95% and 99% confidence intervals (for clinical and resilience features, respectively) did not cross zero were considered significant, suggesting that they were stable across different sampling cohorts.

Explore the sex difference in resilience effect

Many studies show that normal women with elevated Aβ are more vulnerable to episodic memory decline than men [21]. Whether sex have a moderation effect in AD neuropathology? Here, we integrate the synergetic effect of sex and A/T-specific effect in the model, which allows us to investigate the possible sex difference in moderating the neurodegenerative procession. To do so, we add a three-way interaction to the brain regions where A/T-specific resilience has been found in one of the statistical models above. For example, suppose we find the education-by-Aβ interaction term satisfies the resilience definition. We can add the eduction-by-Aβ-sex term into the underlying model and examine whether the new three-way interaction term exhibits significance. The sign of the corresponding effect size allows us to determine whether males or females have the advantage to neuropathology burden at the particular brain region.

Table 3
The statistical summary of the nodes with significant A-specific resilience w.r.t. eduction

Region name	$\beta_{Amyloid \times Mid\_Edu}$ (Standard Error)	Unadjusted p	$\beta_{Amyloid \times High\_Edu}$ (Standard Error)	Unadjusted p
L. angular gyrus	0.034 (0.031)	0.265	0.059 (0.029)	**0.043***
L. superior parietal lobule	0.055 (0.026)	**0.038***	0.042 (0.025)	0.091
R. angular gyrus	0.031 (0.032)	0.320	0.082 (0.030)	**0.005***

*The significant level is 95% and the sample size is 1,086.

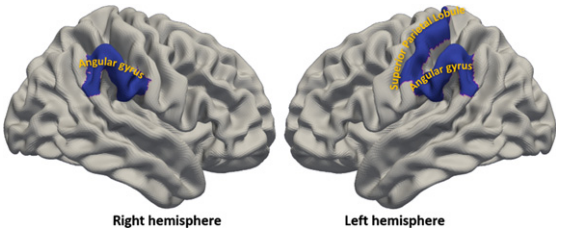

Fig. 2. The brain regions bear A-specific resilience w.r.t. education.

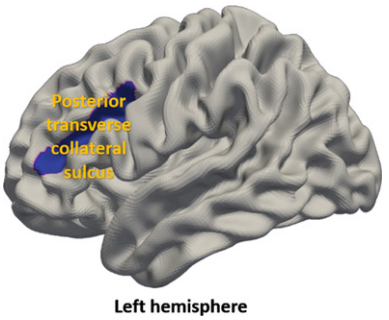

Fig. 3. Only left posterior transverse collateral sulcus bears the T-specific resilience w.r.t. eduction.

RESULTS

A/T-specific resilience effect underlying SES factors

First, we examine the A-specific resilience effect by applying the statistical models in Equation 1-2 to 148 brain regions. The statistical testing results of A-specific resilience w.r.t. eduction are summarized in Table 3, where the regions that satisfy our resilience definition (not only pathology-by-eduction interaction show significance but also the effect size has positive value) are shown. Specifically, we observed significant effects ($p < 0.05$) of Aβ at 47 nodes. Among these regions, three regions (L/R angular gyrus and L. superior parietal lobule) showed the significant A-specific resilience effect from higher education (either at medium or high education level), as shown in Fig. 2. However, no nodes were observed having A-specific resilience w.r.t. occupation.

Second, we examine the T-specific resilience for each brain region with regards to education and occupation using the statistical models in Equation 3-4, respectively. Similarly, we display the statistical testing results for the regions satisfying our resilience definition in Table 4. We observed Tau pathology exhibit significant resilience effects ($p < 0.05$) at 61 brain regions. On top of this, only one region (posterior transverse collateral sulcus) in the left hemisphere T-resilience w.r.t. education, which is shown in Fig. 3. Two regions, both from the right hemisphere, are found associated with T-resilience w.r.t. occupation, which are shown in Fig. 4.

Since the non-linear model is not employed in this work, we performed the linear assumption diagnosis and found some extreme outliers. After we conduct a sensitivity analysis removing all the extreme outliers, all discoveries regarding the biomarker-specific resilience remain the same.

Table 4
The summary statistics of the nodes with significant T-resilience w.r.t education and occupation

SES factor	Region name	$\beta_{Tau \times Mid\_SES}$ (Standard Error)	Unadjusted p	$\beta_{Tau \times High\_SES}$ (Standard Error)	Unadjusted p
Education	*L. posterior transverse collateral sulcus*	0.105 (0.051)	**0.041***	0.120 (0.048)	**0.013***
Occupation	*R. posterior transverse collateral sulcus*	0.096 (0.060)	0.111	0.097 (0.041)	**0.017***
	R. lateral occipito-temporal sulcus	0.079 (0.036)	**0.030***	0.040 (0.030)	0.188

*The significant level is 95% and the sample size is 346.

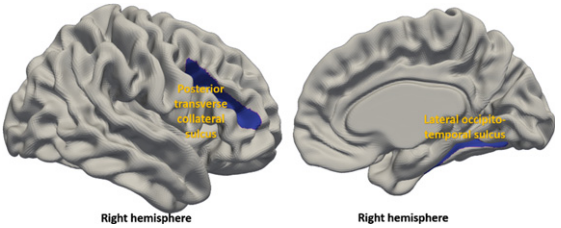

Fig. 4. Two brain regions (R. posterior transverse collateral sulcus and R. lateral occipitotemporal sulcus) bear the T-specific resilience w.r.t. occupation.

Genetic association analysis with neuroplastic markers

Among the selected BDNF SNPs (Table 5), only rs10835211 was found to be statistically associated with A-specific resilience score (w.r.t. education) at the left/right angular gyrus and left superior parietal lobule. The angular gyrus is involved in processing concepts [22] and superior parietal lobule is related to working memory and visual perception.

Due to the limited sample size, however, rs10835211 fails to survive the False Discovery Rate (FDR) correction. The detail of statistical results is summarized in Table 6. By examing the Lucas-zoom plot (Fig. 5), there is a clear sign that rs10835211 is much more correlated to the resilience effect than other SNPs.

Linked dimensions between clinical symptom to the identified A-specific resilience effect

Due to the sample size, we only used the identified A-specific resilience effect to link the itemized cognitive outcomes shown in Table 2. Based on the scree plot of covariance explained, we selected the first two canonical variates for further analysis. The significance of each of these linked dimensions of cognitive outcome and resilience was assessed using a permutation test. FDR was used to control for type I error rate due to multiple testing. Of the top two canonical variates, both were significant (canonical variate #1: Pearson correlation $r = 0.13$, P_{FDR}=0.008; canonical variate #2: $r = 0.12$, P_{FDR}=0.016). The resampling procedure revealed that 4 of those 22 clinical outcomes reliably contributed to at least one of the two linked dimensions. These cognitive outcomes were the learning evaluation in RAVLT, a measure of verbal memory. Many patients with mild cognitive impairment begin to show episodic memory deficits early in their clinical course. Higher cognitive reserve has also been found to be associated with improved episodic memory in older adults [23]. The total participant everyday cognition score as well as the memory and organization domains of the study partner report on the everyday cognition test. The everyday cognition test assesses mild functional changes that are associated with early cognitive deficits. A previous model in patients with subjective cognitive decline found a strong association between the executive function domain of everyday cognition and tau as well as the memory domain and Aβ [24]. Specifically, we mapped these data-driven items to typical clinical diagnostic categories, as shown in Fig. 6. It is clear that the first linked dimension implies that the identified A-specific resilience is not only associated with the total score on the Ecog test (sCCA coefficient: 0.38) in general but also correlated with two specific items (study partner memory: sCCA coefficient 0.48; study partner organization: sCCA coefficient 0.67) in

Table 5
BDNF SNP location and information details

SNP	Major/ Minor	Minor Allele Frequency	Chromosome Position[a]	Inter-marker Distance[b]	Location
rs11030094	A/G	10.3%	27659775	0	Intergenic
rs925946	T/G	40.4%	27667202	7,427	Intergenic
rs10501087	T/C	39.8%	27670108	2,906	Intergenic
rs2203877	T/C	9.1%	27670910	802	Intergenic
rs6265	C/T	36.1%	27679916	9,006	Nonsynonymous
rs11030104	A/G	39.9%	27684517	4,601	Intron
rs11030108	G/A	40.0%	27695464	10,947	Intron
rs10835211	G/A	**47.7%**	**27701365**	**5,901**	**Intron**
rs7934165	G/A	4.2%	27731983	30,618	Intron
rs1157659	T/C	7.2%	27741419	9,436	Intergenic
rs12273363	T/C	39.7%	27744859	3,440	Upstream
rs908867	C/T	17.3%	27745764	905	Upstream
rs1491850	T/C	15.4%	27749725	3,961	Intergenic

[a]Chromosome 11 position according to NCBI Build 37.1 genome assembly, [b]In base pairs.

Table 6
The summary statistics of association analysis of between *rs10835211* and A-specific resilience scores

Regions	Effect size	*p*	Adjusted *p*
L. angular gyrus	0.228 (0.091)	0.012	0.120
L. superior parietal lobule	0.244 (0.092)	0.0080	0.077
R. angular gyrus	0.242 (0.093)	0.0094	0.090

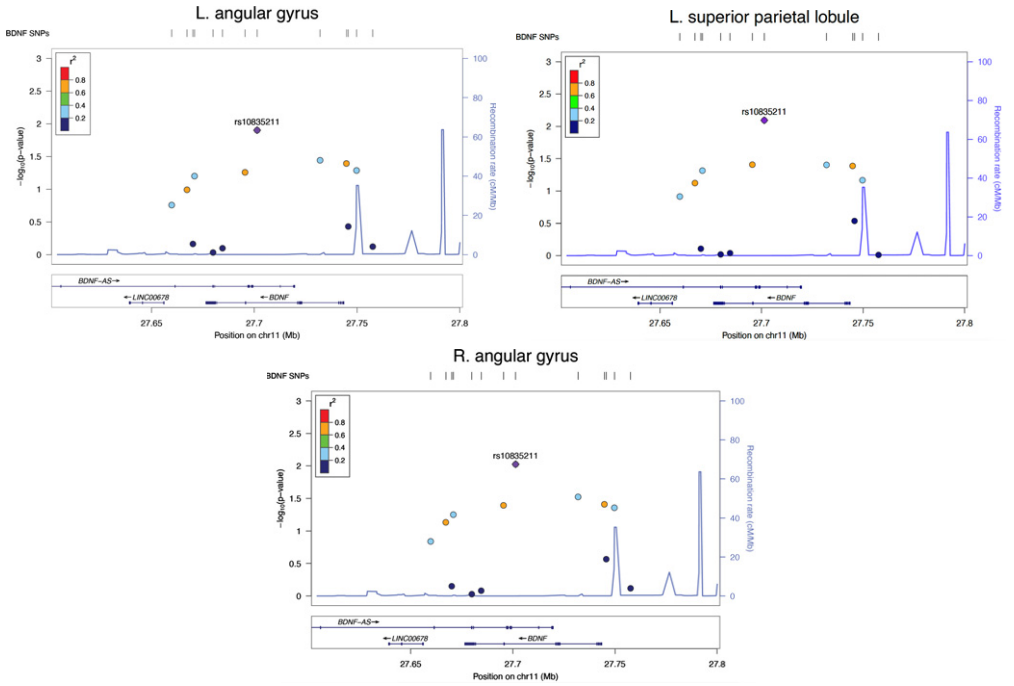

Fig. 5. Locus-zoom plots of *BDNF*-SNP-significant signals in L. angular gyrus, L. superior parietal lobule, R. angular gyrus. Genomic position is depicted on the x-axis. The y-axis shows the –log(10) of the *p*-value.

the Ecog test, where the sCCA coefficients reflect the correlations between resilience effect and the clinical outcome. In the second linked dimension, it seems that RAVLT learning score (sCCA coefficient: 0.73) is a more predominant factor than Ecog study partner organization score (sCCA coefficient: 0.39). It is worth noting that the A-specific resilience effect under investigation is associated with education level. This suggests that subjects have resilience to changes in their memory and everyday cognition. Cognitive reserve has been found to decrease risk of dementia even in patients with subjective cognitive decline, suggesting that resilience in everday cognition may be an important marker for decreased progression to clinical AD [25].

The sex difference in resilience effect

First, we examine the sex difference in A-specific resilience effect through the sex-by-resilience interaction in our model. The statistical testing results of sex differences in A-specific resilience w.r.t. eduction are summarized in Table 7, where only display the regions showing significant sex differences in resilience effect. Four regions (L/R superior parietal lobule, L. precuneus, and L. subcallosal gyrus) showed the significant sex difference in A-specific resilience effect from higher education. Similarly, three regions (L. precuneus, L. superior occipital gyrus, and R. superior parietal lobule) were observed the significant sex difference in A-specific resilience effect from occupation.

Second, we examined the sex difference in T-specific resilience for each brain region w.r.t. to education and occupation. Similarly, we display the statistical testing results for the regions showing significant sex differences in Table 8. R. collateral sulcus in the middle of the right hemisphere showed significant sex differences in both T-resilience w.r.t education and occupation.

Table 7
The statistical summary of the nodes with significant gender difference in A-resilience w.r.t education and occupation

SES factor	Region name	β $Amyloid\times Mid\_SES \times Male$ (Standard Error)	p	β $Amyloid\times High\_SES \times Male$ (Standard Error)	p
Education					
	L. Superior parietal lobule	–0.109 (0.054)	**0.042**	–0.100 (0.051)	0.051
	L. Precuneus	–0.130 (0.048)	**0.006**	–0.114 (0.046)	**0.013**
	L. Subcallosal gyrus	–0.035 (0.048)	0.4676	–0.116 (0.047)	**0.014**
	R. Superior parietal lobule	–0.135 (0.055)	**0.015**	–0.096 (0.052)	0.064
Occupation					
	L. Precuneus	–0.162 (0.048)	**0.028**	–0.146 (0.046)	**0.038**
	L. Superior occipital gyrus	–0.261 (0.117)	**0.026**	–0.199 (0.114)	0.0821
	R. Transverse temporal gyrus	–0.222 (0.112)	**0.048**	–0.149 (0.107)	0.163

*The significant level is 95% and the sample size is 1086.

Table 8
The statistical summary of the nodes with significant gender difference in T-resilience w.r.t education and occupation

SES factor	Region name	β $Tau\times Mid\_SES \times Male$ (Standard Error)	p	β $Tau\times High\_SES \times Male$ (Standard Error)	p
Education					
	R. Collateral sulcus middle RH	–0.097 (0.061)	0.114	–0.111 (0.052)	**0.033**
Occupation					
	R. Collateral sulcus middle RH	–0.130 (0.099)	0.189	–0.303 (0.083)	**0.0003**

*The significant level is 95% and the sample size is 346.

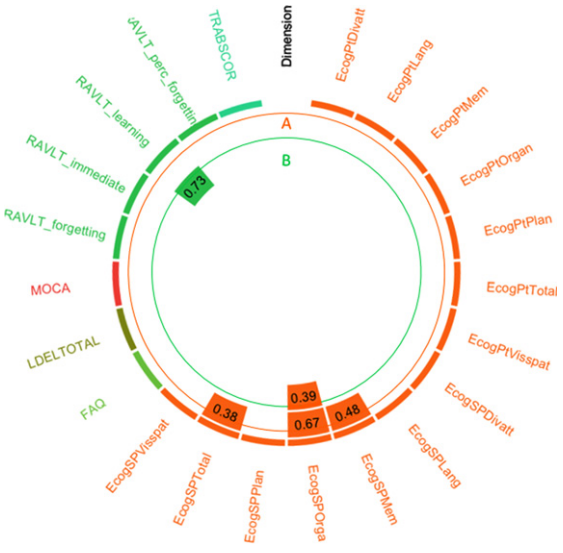

Fig. 6. The linked dimensions between A-specific resilience and itemized clinical outcomes. The outer and inter rings correspond to the first linked dimension (top canonical variate) and the second linked dimension, respectively. It is clear that the first linked dimension consists of three factors (EcogSPTotal, EcogSPOrga, and EcogSPMem) and the second linked dimension consists of two major factors (RAVLT_Learning and EcogSPOrga), where the sCCA coefficients indicate the correlation between resilience effect and the underlying clinical outcome.

DISCUSSION

A major challenge in the care and management of AD is the paradoxical relationship between the burden of AD pathology and its clinical outcome [5, 26]. Recent evidence shows cognitive reserve, the brain's capability to preserve cognition despite underlying AD pathology, is a key determinant that moderates clinical progression [5–8, 16, 26–28]. In this context, it is of high demand to understand the neurobiological basis of brain resilience and the multi-factorial role of environmental factors such as education. Importantly, the unprecedented amount of longitudinal neuroimaging data allows us to investigate the effect of brain resilience in cognitive decline, which sets the stage for precision medicine of AD treatment.

In this study, we present a novel computational measurement to characterize the regional resilience underlying the mechanistic pathway of A-T-N biomarkers. We have identified several brain regions that manifest resilience to Aβ and tau biomarkers. Furthermore, we have identified resilience effects that are potentially correlated with rs10835211 SNP of the BDNF gene. The sCCA analysis is used to establish the link between resilience and cognitive

outcomes. We found that cognitive measures of learning and memory demonstrate resilience, which is aligned with previous studies of the cognitive reserve [29].

Mounting evidence shows that APOE manifests sex-specific patterns through neuroimaging data and cerebrospinal fluid biomarkers of Aβ and tau [30, 31]. However, the mechanism of how sex-specific interaction exerts the resilience effect on AD risk and putative endophenotypes with a clear genetic connection is largely elusive. As a pilot study, we further examine the sex differences at the brain regions showing resilience to the pathological burden by evaluating the joint effect between sex and identified resilience measurements. Although the joint effect does not show the significant difference between males and females, the estimated effect size of the interaction terms is negative in all testings, which implies females with higher education or better occupation might have the advantage in moderate the pathological burden.

ACKNOWLEDGMENTS

This work was supported by the National Institutes of Health AG049089, AG059065, AG073927, and AG068399.

Data collection and sharing for this project was funded by the Alzheimer's Disease Neuroimaging Initiative (ADNI) (National Institutes of Health Grant U01 AG024904) and DOD ADNI (Department of Defense award number W81XWH-12-2-0012). ADNI is funded by the National Institute on Aging, the National Institute of Biomedical Imaging and Bioengineering, and through generous contributions from the following: AbbVie, Alzheimer's Association; Alzheimer's Drug Discovery Foundation; Araclon Biotech; BioClinica, Inc.; Biogen; Bristol-Myers Squibb Company; CereSpir, Inc.; Cogstate; Eisai Inc.; Elan Pharmaceuticals, Inc.; Eli Lilly and Company; EuroImmun; F. Hoffmann-La Roche Ltd and its affiliated company Genentech, Inc.; Fujirebio; GE Healthcare; IXICO Ltd.; Janssen Alzheimer Immunotherapy Research & Development, LLC.; Johnson & Johnson Pharmaceutical Research & Development LLC.; Lumosity; Lundbeck; Merck & Co., Inc.; Meso Scale Diagnostics, LLC.; NeuroRx Research; Neurotrack Technologies; Novartis Pharmaceuticals Corporation; Pfizer Inc.; Piramal Imaging; Servier; Takeda Pharmaceutical Company; and Transition Therapeutics. The Canadian Institutes of Health Research is providing funds to support ADNI clinical sites in Canada. Private sector contributions are facilitated by the Foundation for the National Institutes of Health (http://www.fnih.org). The grantee organization is the Northern California Institute for Research and Education, and the study is coordinated by the Alzheimer's Therapeutic Research Institute at the University of Southern California. ADNI data are disseminated by the Laboratory for Neuro Imaging at the University of Southern California.

Authors' disclosures available online (https://www.j-alz.com/manuscript-disclosures/21-5160r1).

REFERENCES

[1] Jack CR, Bennett DA, Blennow K, Carrillo MC, Dunn B, Haeberlein SB, Holtzman DM, Jagust W, Jessen F, Karlawish J, Liu E, Molinuevo JL, Montine T, Phelps C, Rankin KP, Rowe CC, Scheltens P, Siemers E, Snyder HM, Sperling R, Elliott C, Masliah E, Ryan L, Silverberg N (2018) NIA-AA Research Framework: Toward a biological definition of Alzheimer's disease. *Alzheimers Dement* **14**, 535-562.

[2] Jack CR, Knopman DS, Jagust WJ, Petersen RC, Weiner MW, Aisen PS, Shaw LM, Vemuri P, Wiste HJ, Weigand SD, Lesnick TG, Pankratz VS, Donohue MC, Trojanowski JQ (2013) Tracking pathophysiological processes in Alzheimer's disease: An updated hypothetical model of dynamic biomarkers. *Lancet Neurol* **12**, 207-216.

[3] Jack CR, Lowe VJ, Weigand SD, Wiste HJ, Senjem ML, Knopman DS, Shiung MM, Gunter JL, Boeve BF, Kemp BJ, Weiner M, Petersen RC (2009) Serial PIB and MRI in normal, mild cognitive impairment and Alzheimer's disease: Implications for sequence of pathological events in Alzheimer's disease. *Brain* **132** (Pt 5), 1355-1365.

[4] Jack CR, Holtzman DM (2013) Biomarker modeling of Alzheimer's disease. *Neuron* **80**, 1347-1358.

[5] Stern Y (2002) What is cognitive reserve? Theory and research application of the reserve concept. *J Int Neuropsychol Soc* **8**, 448-460.

[6] Stern Y (2006) Cognitive reserve and Alzheimer disease. *Alzheimer Dis Assoc Disord* **20**, 112-117.

[7] Stern Y (2012) Cognitive reserve in ageing and Alzheimer's disease. *Lancet Neurol* **11**, 1006-1012.

[8] van Loenhoud AC, Wink AM, Groot C, Verfaillie SCJ, Twisk J, Barkhof F, van Berckel B, Scheltens P, van der Flier WM, Ossenkoppele R (2017) A neuroimaging approach to capture cognitive reserve: Application to Alzheimer's disease. *Hum Brain Mapp* **38**, 4703-4715.

[9] Anatürk M, Kaufmann T, Cole JH, Suri S, Griffanti L, Zsoldos E, Filippini N, Singh-Manoux A, Kivimäki M, Westlye LT, Ebmeier KP, de Lange A-MG (2021) Prediction of brain age and cognitive age: Quantifying brain and cognitive maintenance in aging. *Hum Brain Mapp* **42**, 1626-1640.

[10] Zhang Y, Hao Y, Li L, Xia K, Wu G (2020) A novel computational proxy for characterizing cognitive reserve in Alzheimer's disease. *J Alzheimers Dis* **78**, 1217-1228.

[11] (2020) 2020 Alzheimer's disease facts and figures. *Alzheimers Dement* **16**, 391-460.

[12] Destrieux C, Fischl B, Dale A, Halgren E (2010) Automatic parcellation of human cortical gyri and sulci using standard anatomical nomenclature. *Neuroimage* **53**, 1-15.

[13] Lo RY, Jagust WJ, Alzheimer's Disease Neuroimaging Initiative (2013) Effect of cognitive reserve markers on Alzheimer pathologic progression. *Alzheimer Dis Assoc Disord* **27**, 343-350.

[14] Rose D, Pevalin DJ (2003) *A Researcher's Guide to the National Statistics Socio-economic Classification.* SAVE Publications Ltd.

[15] Wilms I, Croux C (2015) Sparse canonical correlation analysis from a predictive point of view. *Biom J* **57**, 834-851.

[16] Stern Y (2017) An approach to studying the neural correlates of reserve. *Brain Imaging Behav* **11**, 410-416.

[17] Knüsel B, Beck KD, Winslow JW, Rosenthal A, Burton LE, Widmer HR, Nikolics K, Hefti F (1992) Brain-derived neurotrophic factor administration protects basal forebrain cholinergic but not nigral dopaminergic neurons from degenerative changes after axotomy in the adult rat brain. *J Neurosci* **12**, 4391-4402.

[18] Caspers S, Röckner ME, Jockwitz C, Bittner N, Teumer A, Herms S, Hoffmann P, Nöthen MM, Moebus S, Amunts K, Cichon S, Mühleisen TW (2020) Pathway-specific genetic risk for Alzheimer's disease differentiates regional patterns of cortical atrophy in older adults. *Cereb Cortex* **30**, 801-811.

[19] Kaufman SK, Sanders DW, Thomas TL, Ruchinskas AJ, Vaquer-Alicea J, Sharma AM, Miller TM, Diamond MI (2016) Tau prion strains dictate patterns of cell pathology, progression rate, and regional vulnerability *in vivo*. *Neuron* **92**, 796-812.

[20] Hardoon DR, Shawe-Taylor J (2011) Sparse canonical correlation analysis. *Machine Learn* **83**, 331-353.

[21] Lindbergh CA, Casaletto KB, Staffaroni AM, La Joie R, Iaccarino L, Edwards L, Tsoy E, Elahi F, Walters SM, Cotter D, You M, Apple AC, Asken B, Neuhaus J, Rexach JE, Wojta KJ, Rabinovici G, Kramer JH (2020) Sex-related differences in the relationship between β-amyloid and cognitive trajectories in older adults. *Neuropsychology* **34**, 835-850.

[22] Seghier ML (2013) The angular gyrus: Multiple functions and multiple subdivisions. *Neuroscientist* **19**, 43-61.

[23] Mohammad N, Rezapour T, Kormi-Nouri R, Abdekhodaie E, Ghamsari AM, Ehsan HB, Hatami J (2020) The effects of different proxies of cognitive reserve on episodic memory performance: Aging study in Iran. *Int Psychogeriatr* **32**, 25-34.

[24] Shokouhi S, Conley AC, Baker SL, Albert K, Kang H, Gwirtsman HE, Newhouse PA, Alzheimer's Disease Neuroimaging Initiative (2019) The relationship between domain-specific subjective cognitive decline and Alzheimer's pathology in normal elderly adults. *Neurobiol Aging* **81**, 22-29.

[25] Jia F, Li Y, Li M, Cao F (2021) Subjective cognitive decline, cognitive reserve indicators, and the incidence of dementia. *J Am Med Dir Assoc* **22**, 1449-1455.e1444.

[26] van Loenhoud AC, van der Flier WM, Wink AM, Dicks E, Groot C, Twisk J, Barkhof F, Scheltens P, Ossenkoppele R (2019) Cognitive reserve and clinical progression in Alzheimer disease. *Neurology* **93**, e334.

[27] Reed BR, Mungas D, Farias ST, Harvey D, Beckett L, Widaman K, Hinton L, DeCarli C (2010) Measuring cognitive reserve based on the decomposition of episodic memory variance. *Brain* **133**, 2196-2209.

[28] Medaglia JD, Pasqualetti F, Hamilton RH, Thompson-Schill SL, Bassett DS (2017) Brain and cognitive reserve: Translation via network control theory. *Neurosci Biobehav Rev* **75**, 53-64.

[29] Sundermann EE, Maki PM, Rubin LH, Lipton RB, Landau S, Biegon A (2016) Female advantage in verbal memory: Evidence of sex-specific cognitive reserve. *Neurology* **87**, 1916-1924.

[30] Barnes LL, Wilson RS, Bienias JL, Schneider JA, Evans DA, Bennett DA (2005) Sex differences in the clinical manifestations of Alzheimer disease pathology. *Arch Gen Psychiatry* **62**, 685-691.

[31] Farrer LA, Cupples LA, Haines JL, Hyman B, Kukull WA, Mayeux R, Myers RH, Pericak-Vance MA, Risch N, van Duijn CM (1997) Effects of age, sex, and ethnicity on the association between apolipoprotein E genotype and Alzheimer disease: A meta-analysis. *JAMA* **278**, 1349-1356.